Charge-density wave and three-dimensional Fermi surface in $1T$-$TaSe_2$ studied by photoemission spectroscopy

K. Horiba, K. Ono,* J. H. Oh, T. Kihara, S. Nakazono, and M. Oshima
Department of Applied Chemistry, University of Tokyo, Tokyo 113-8656, Japan

O. Shiino
Data Storage Technology Center, TDK Corporation, Saku 385-0009, Japan

H. W. Yeom
Atomic Scale Surface Science Research Center and Department of Physics, Yonsei University, Seoul 120-749, Korea

A. Kakizaki
Institute for Solid State Physics, University of Tokyo, Kashiwa 277-8581, Japan

Y. Aiura
National Institute of Advanced Idustrial Science and Technology, Tsukuba 305-8568, Japan
(Received 11 April 2002; revised manuscript received 3 June 2002; published 9 August 2002)

We have investigated the electronic structure of the commensurate charge-density-wave (CDW) phase for $1T$-$TaSe_2$ by Ta $4f$ core-level and the angle-resolved photoemission. From the energy shifts of Ta $4f$ core levels due to a CDW formation, it is found that the CDW amplitude in the $1T$-$TaSe_2$ is smaller than that in $1T$-TaS_2 reported previously. The band dispersion along the normal to the two-dimensional layers indicates that $1T$-$TaSe_2$ has a three-dimensional (3D) character in the Fermi surface compared with $1T$-TaS_2, which has a two-dimensional Fermi surface. The 3D Fermi surface of $1T$-$TaSe_2$ is thought to originate from the larger interaction between layers due to a large charge transfer between Ta $5d$ and Se $4p$ orbitals.

DOI: 10.1103/PhysRevB.66.073106 PACS number(s): 79.60.Bm, 71.20.−b

The layered transition metal dichalcogenides, $1T$-TaS_2 and $1T$-$TaSe_2$ have attracted much attention because of their various unique physical properties related to the formation of a charge density wave (CDW).[1] Both materials have the same CdI_2-type structure with the space group D_{3d}^3. Ta atoms form a hexagonal sheet and are sandwiched between sheets of hexagonally arranged chalcogen (Se and S) atoms as shown in Fig. 1(a). The bulk Brillouin zone and the high-symmetry line are also shown in Fig. 1(b). Although these two materials have very similar crystal structures, chemical structures and CDW superstructures, they exhibit drastically different physical properties. Figure 1(c) shows a temperature dependence of electric resistivity for $1T$-$TaSe_2$ and $1T$-TaS_2 single crystals measured by a standard four-probe method.[2] As shown in Fig. 1(c), $1T$-TaS_2 shows two successive first-order transitions; incommensurate CDW (ICDW) to nearly commensurate CDW (NCCDW) transition at about 350 K and NCCDW to commensurate CDW (CCDW) transition at about 180 K. A metal-to-insulator transition occurs followed by NCCDW to CCDW transition. On the other hand, $1T$-$TaSe_2$ shows an incommensurate CDW to CCDW transition at about 430 K and no drastic change of an electrical conductivity in the whole CCDW phase, and exhibits a metallic behavior.

In order to understand the physical properties, the electronic structures of $1T$-TaS_2 have been intensively studied by various techniques, such as scanning tunneling spectroscopy (STS),[3,4] angle-resolved photoemission spectroscopy (ARPES),[5–8] and angle-resolved inverse photoemission spectroscopy.[9] It is found that an energy gap of about 200 meV is opened at the Fermi energy (E_F) in the CCDW phase. The formation of the correlation gap in the CCDW phase of $1T$-TaS_2 is considered to be due to the Mott localization[10]. On the other hand, the electronic structures of $1T$-$TaSe_2$ have also been investigated by STS (Refs. 11,12) and photoemission.[13] In the STS study of $1T$-$TaSe_2$, a finite density of state (DOS) exists at E_F in the CCDW phase,

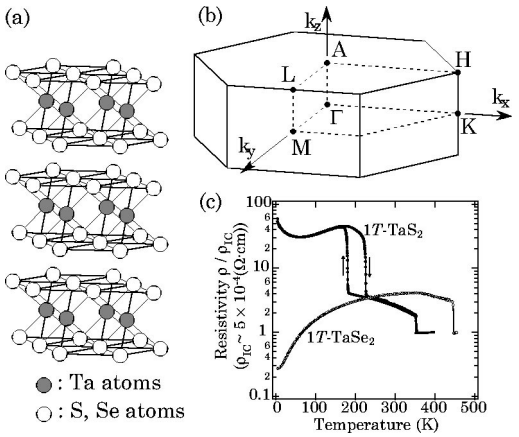

FIG. 1. (a) The CdI_2-type crystal structure of $1T$-TaS_2 and $1T$-$TaSe_2$. Ta atoms form a hexagonal sheet and are sandwiched between sheets of hexagonally arranged chalcogen (Se and S) atoms. (b) Schematic diagram of the bulk Brillouin zone for the CdI_2-type structure and the high-symmetry line. (c)Temperature dependence of resistivity for $1T$-TaS_2 and $1T$-$TaSe_2$. The resistivity is normalized with the resistivity in ICDW phase.

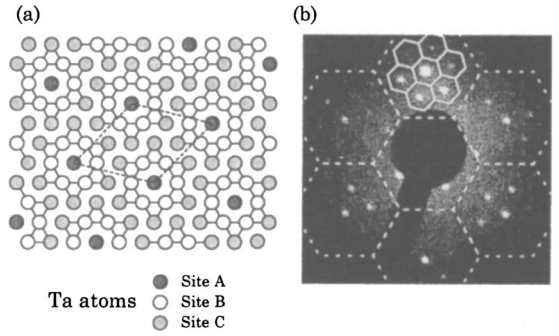

FIG. 2. (a) Schematic model of Ta atoms in the $\sqrt{13}\times\sqrt{13}$ "star of David" CCDW superstructure. There are three Ta sites due to the difference in a charge population. (b) LEED pattern of the $\sqrt{13}\times\sqrt{13}$ superstructure in $1T$-$TaSe_2$. Dotted lines show 1×1 surface Brillouin zone of $1T$-$TaSe_2$ and solid lines show the surface Brillouin zone for a $\sqrt{13}\times\sqrt{13}$ superstructure. The superlattice reflections due to CDW induced superstructure are observed in center of the $\sqrt{13}\times\sqrt{13}$ surface Brillouin zone.

indicating the metallic characteristics of $1T$-$TaSe_2$. However, the detailed momentum-dependent electronic structure of $1T$-$TaSe_2$ has been not understood yet.

In this report, we have investigated the electronic structure of the CCDW phase of $1T$-$TaSe_2$ in detail from the CDW-induced core-level shift of Ta $4f$ and the valence band dispersion using ARPES. Single crystals of $1T$-$TaSe_2$ were grown by the iodine transport method. Photoemission measurements were carried out using an angle-resolved photoemission spectrometer (VG Microtech; ARUPS10) at the BL-1C of the Photon Factory (PF).[14] The samples were cleaved *in situ* in ultra high vacuum. The base pressure was in the order of 10^{-10} Torr. The sample orientation and the CDW-induced superstructure as well as the surface quality were monitored by low-energy electron diffraction (LEED). High-resolution core-level photoemission spectra of Ta $4f$ were taken at the photon energy of 80eV at room temperature (RT) and 20 K. ARPES was performed along the high-symmetry Γ-A direction of a $1T$-$TaSe_2$ Brillouin zone, which is shown in Fig. 1(b). The band dispersions along the Γ-A direction were measured by changing the photon energy from 20 to 35 eV at the normal emission. The angular resolution of the photoemission measurements was about $\pm2°$. All the ARPES measurements were performed at RT and the total energy resolution was about 100 meV. High-resolution angle-resolved photoemission measurements along the Γ-A direction were also performed using another photoemision spectrometer (Gammadata Scienta SES100) at the normal incident monochromator beamline BL-20A of the PF. The measurements temperature was about 20 K and the total energy resolution and angular resolution were about 20 meV and about $\pm0.2°$, respectively.

In the CCDW phase of $1T$-$TaSe_2$, Ta atoms are periodically displaced followed by the CDW formation and 13 Ta atoms form, the so-called "star of David" cluster as shown in Fig. 2(a).[1] This leads to a $\sqrt{13}\times\sqrt{13}$ CDW-induced supercell, which is rotated by 13.9° from the 1×1 unit cell. Figure 2(b) shows a LEED pattern of $1T$-$TaSe_2$ at RT. Clear

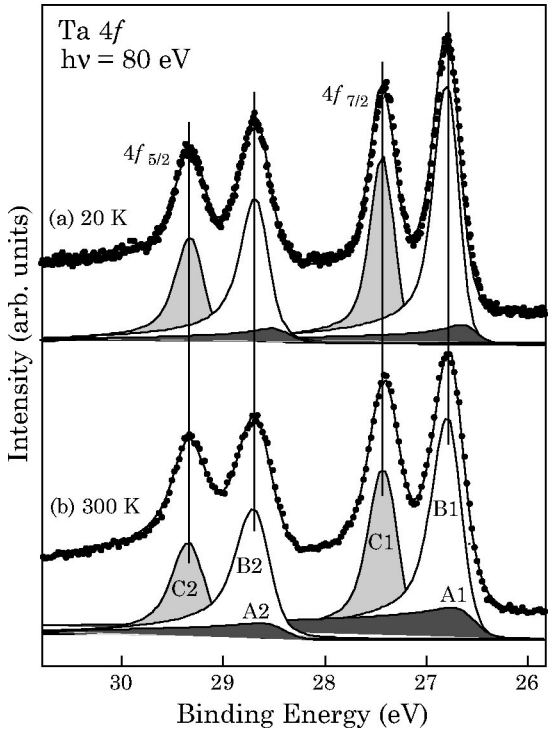

FIG. 3. High-resolution photoemission spectra of Ta $4f$ core levels for $1T$-$TaSe_2$ (a) at 20 K and (b) RT.

$\sqrt{13}\times\sqrt{13}$ diffraction spots due to the CDW superstructure are observed, indicating the sample is in the well-developed CCDW phase.

In a $\sqrt{13}\times\sqrt{13}$ CDW superstructure of $1T$-$TaSe_2$, as shown in Fig. 2(a), there are three different Ta sites, namely, site A with one atom, and sites B and C with six atoms each, due to the difference in local charge densities.[15,16] At the site A and B with a larger local charge density, the screening effect of a photohole created by photoemission is stronger and the binding energy shifts toward the lower energy side.[16,17] Figure 3 show the high-resolution photoemission spectra of Ta $4f$ core levels at 20 K (a) and at RT (b). The spin-orbit-split doublet ($\Delta E_{SO}\sim1.90\pm0.10$ eV) is split into a further triplet which corresponds to three different Ta sites A, B, and C. The peaks show asymmetric line shapes. We fitted the peaks using six Doniach-Sunjic line shapes[18] and obtained the optimal fitting results. The parameters used for the optimal fitting are shown in Table I. The CDW-induced core-level shift of $1T$-$TaSe_2$ ($\Delta E_{CDW}=E_B-E_C$) is 0.65 ± 0.01 eV, which is smaller than the corresponding shift of $1T$-TaS_2 of 0.70 ± 0.01 eV.[16,17,19] The CDW-induced shift corresponds to the magnitude of the difference in electron density between site-B and site-C and is directly connected with the amplitude of CDW. It is suggested that the amplitude of CDW in $1T$-$TaSe_2$ is slightly smaller than that in $1T$-TaS_2.

In $1T$-TaS_2, a drastic temperature dependence of the spectral line-shape was observed due to a temperature-dependent growth of the CCDW domains.[6,19] The metal-to-insulator transition of $1T$-TaS_2 is closely related to the growth of the commensurate domains in the nearly commensurate phase,

TABLE I. Fitting parameters of six components for Ta $4f$ core-level photoemission spectra.

Peak		$A1$	$B1$	$C1$	$A2$	$B2$	$C2$
Binding energy (eV)		22.42	22.65	23.29	24.31	24.57	25.22
Gaussian width (eV)	RT	0.29	0.29	0.29	0.29	0.29	0.29
	20 K	0.24	0.24	0.24	0.24	0.24	0.24
Lorenzian width (eV)		0.04	0.04	0.04	0.11	0.11	0.11
Singularity	RT	0.79	0.20	0.16	0.79	0.20	0.16
	20 K	0.59	0.17	0.13	0.59	0.17	0.13

as the temperature decreases. On the other hand, in $1T$-$TaSe_2$, no drastic change in the spectral line shape of Ta $4f$ between RT and 20 K was observed, that is contrary to the previous report.[20] Compared with the ΔE_{CDW} from the spectra taken at RT and 20 K, there is no temperature dependence, indicating that the amplitude of CDW in $1T$-$TaSe_2$ remains constant in the whole temperature range of CCDW phase.

Figure 4(a) shows the band dispersion along the Γ-A direction of the $1T$-$TaSe_2$ Brillouin zone [Fig. 1(b)]. We have observed two flat bands at the binding energies of 0.2 eV and 0.8 eV (Fig. 4; open triangles). In addition, we have observed a band, which crosses E_F (Fig. 4; filled triangles) with a dispersion of about 300 meV. This band crosses the E_F at the photon energies of 22 ± 1 eV, ($k_\perp=-0.25\pm0.04$ Å^{-1}), and 32 ± 1 eV ($k_\perp=0.25\pm0.04$ Å^{-1}). The E_F crossing between the photon energies of 22 and 23 eV is more clearly observed in the high-resolution photoemission measurements shown in Fig. 4(b). The bottom of the band (Γ point, $k_\perp=0$) is located at the photon energy of 27 eV. In contrast, it is observed very recently that $1T$-TaS_2 has no such band with a noticeable dispersion along the $k_\perp$ direction and no band crosses to E_F.[8] It is thus concluded that $1T$-$TaSe_2$ has a three-dimensional (3D) Fermi surface, whereas $1T$-TaS_2 has a two-dimensional (2D) Fermi surface.

Two flat bands shown with open triangles in Fig. 4(a) suggest that the bands incorporate the atomic displacement due to the formation of CDW. A tight-binding band calculation for the CDW phase of $1T$-TaS_2 is reported by Smith *et al.*,[15] where the CCDW band structure is calculated by folding the non-CDW Ta $5d$ band structure toward Brillouin zone boundary of the $\sqrt{13}\times\sqrt{13}$ CCDW superlattice. There are three subbands along the high-symmetry direction, just below E_F, in the range from 0.23 to 0.67 eV, and in the range from 0.74 to 1.13 eV. At the Γ point, the calculation predict two peaks in the spectrum at the binding energies of about 0.4 and 0.8 eV. Since the non-CDW Ta $5d$ band structure in $1T$-$TaSe_2$ is very similar to that in $1T$-TaS_2, the calculation seems to be applied to that in $1T$-$TaSe_2$. But we cannot apply this calculation to a band crossing to E_F shown with filled triangles in Fig. 4(a), because of the assumption in this calculation that there is no interlayer interactions.

Other band calculations for the non-CDW state of $1T$-TaS_2 and $1T$-$TaSe_2$ (Refs. 21,22) predicted that

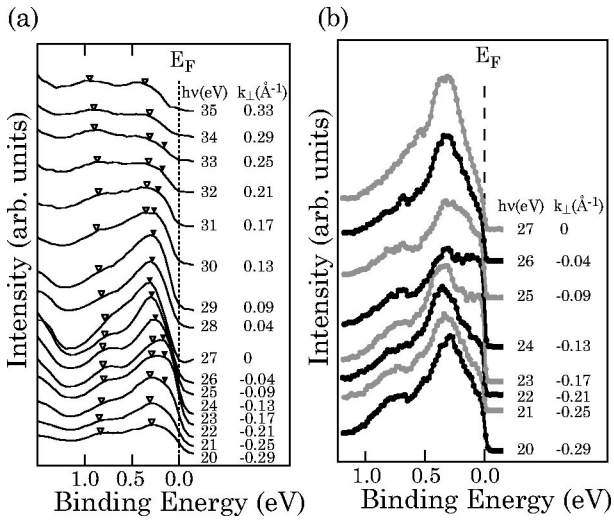

FIG. 4. (a) Angle-resolved photoemission spectra along Γ-A direction. Three subband shown with open and filled triangles were observed. (b) High-resolution angle-resolved photoemission spectra along Γ-A direction. It is clearly observed that a band crosses to E_F between the photon energy of 22 and 23 eV.

$1T$-$TaSe_2$ has stronger interlayer interactions than $1T$-TaS_2 and the Ta $5d$ band crosses E_F between the Γ point and the A point. Our ARPES results agree with the calculation and it is suggested that the strong interlayer interactions remain in the CCDW state of $1T$-$TaSe_2$.

The 3D electronic structure in $1T$-$TaSe_2$ is considered to be due to the larger p-d transfer interactions. Since the $4p$ orbital of the Se ion has a larger spatial extent compared with the $3p$ orbital of S ion, the p-d transfer interaction between chalcogen p orbital and Ta $5d$ orbital in $1T$-$TaSe_2$ becomes larger than that in $1T$-TaS_2. This larger p-d transfer interaction in $1T$-$TaSe_2$ causes a larger interaction between layers and forms a 3D Fermi surface. In the case of $1T$-TaS_2, the origin of the metal-to-insulator transition is considered to be due to the Ta $5d$ electrons that are localized in ''star of David'' clusters as a result of CDW. However, in the case of $1T$-$TaSe_2$, because of the larger interlayer interactions, the electron localization is relatively weak exhibiting metallic character even at a low temperature.

In conclusion, we have observed the electronic structure of the CCDW phase of $1T$-$TaSe_2$ by core-level photoemission spectroscopy and ARPES. The CDW splitting of Ta $4f$ core levels reveals that the CDW amplitude of $1T$-$TaSe_2$ is slightly smaller than that of $1T$-TaS_2. ARPES results along the Γ-A direction indicate that $1T$-$TaSe_2$ has a 3D electronic structure compared with $1T$-TaS_2. The 3D electronic structure observed in $1T$-$TaSe_2$ originates from the larger transfer interaction between Ta $5d$ and Se $4p$ orbitals.

This work was done under Project No. 97S1-002 at Institute of Material Structure Science in KEK, and was partly supported by Grant in Aid for Scientific Research (Grant No. B2-13554012) from Ministry of Education, Culture, Sports, Science and Technology.

*Author to whom all correspondence should be addressed. Electronic address: ono@sr.t.u-tokyo.ac.jp.

[1] J.A. Wilson, F.J. DiSalvo, and S. Mahasan, Adv. Phys. **24**, 117 (1975).
[2] Single crystals of 1*T*-$TaSe_2$ and 1*T*-TaS_2 used for resistivity measurements were grown by the iodine transport method.
[3] J.-J. Kim, W. Yamaguchi, T. Hasegawa, and K. Kitazawa, Phys. Rev. Lett. **73**, 2103 (1994).
[4] J.-J. Kim, C. Park, W. Yamaguchi, O. Shiino, K. Kitazawa, and T. Hasegawa, Phys. Rev. B **56**, 15 573 (1997).
[5] B. Dardel, M. Grioni, D. Malterre, P. Weibel, and Y. Baer, Phys. Rev. B **45**, 1462 (1992).
[6] F. Zwick, H. Berger, I. Vobornik, G. Margaritondo, L. Forro, C. Beeli, M. Onellion, G. Panaccione, A. Taleb-Ibrahimi, and M. Grioni, Phys. Rev. Lett. **81**, 1058 (1998).
[7] Th. Pillo, J. Hayoz, H. Berger, Grioni, L. Schlapbach, and P. Aebi, Phys. Rev. Lett. **83**, 3494 (1999).
[8] Th. Pillo, J. Hayoz, D. Naumovic, H. Berger, L. Gavioli, A. Taleb-Ibrahimi, L. Schlapbach, and P. Aebi, Phys. Rev. B **64**, 245105 (2001).
[9] R. Claessen, B. Burandt, H. Carstensen, and M. Skibowski, Phys. Rev. B **41**, 8270 (1990).
[10] E. Tosatti and P. Fazekas, J. Phys. (France) **37**, C4-165 (1976).
[11] J.-J. Kim, W. Yamaguchi, T. Hasegawa, and K. Kitazawa, Phys. Rev. B **50**, 4958 (1994).
[12] O. Shiino, T. Endo, W. Yamaguchi, H. Sugawara, K. Kitazawa, and T. Hasegawa, Appl. Phys. A: Mater. Sci. Process. **66**, S175 (1998).
[13] K. Horiba, K. Ono, H.W.Yeom.Y. Aiura, O. Shiino, J.H. Oh, S. Nakazono, T. Kihara, M. Oshima, and A. Kakizaki, Physica B **284-288**, 1665 (2000).
[14] K. Ono, J.H. Oh, K. Horiba, M. Mizuguchi, M. Oshima, T. Kiyokura, F. Maeda, Y. Watanabe, A. Kakizaki, T. Kikuchi, A. Yagishita, and H. Kato, Nucl. Instrum. Methods Phys. Res. A **467-468**, 573 (2001).
[15] N.V. Smith, S.D. Kevan, and F.J. DiSalvo, J. Phys. C **18**, 3175 (1985).
[16] H.P. Hughes and J.A. Scarfe, J. Phys.: Condens. Matter **8**, 1457 (1996).
[17] H.P. Hughes and J.A. Scarfe, Phys. Rev. Lett. **74**, 3069 (1995).
[18] S. Doniach and M. Sanjic, J. Phys. C **3**, 285 (1970).
[19] R.A. Pollak, D. Eastman, F.J. Himpsel, P. Heimann, and B. Reihl, Phys. Rev. B **24**, 7435 (1981).
[20] H.P. Hughes and R.A. Pollak, Philos. Mag. **34**, 1025 (1976).
[21] L.F. Mattheiss Phys. Rev. B **8**, 3719 (1973).
[22] A.M. Woolley and G. Wexler, J. Phys. C **10**, 2601 (1977).